One Pot Conversion of Benzophenone Imine into the Relevant 2-Aza-Allenium

Marco Bortoluzzi, Tiziana Funaioli, Fabio Marchetti, Guido Pampaloni, Calogero Pinzino, Stefano Zacchini

Supporting Information

Table of contents

Synthesis and characterization of compounds: general experimental details.

Air/moisture sensitive compounds were manipulated under atmosphere of pre-purified argon using standard Schlenk techniques. The reaction vessels were oven dried at 140°C prior to use, evacuated (10^{-2} mmHg) and then filled with argon. WCl_6 (99.9%, Strem), imines (TCI Europe), $NOBF_4$ (95%, Sigma Aldrich) and deuterated solvents (98+%, Cortecnet) were commercial products stored under argon atmosphere as received. Once isolated, the metal products were conserved in sealed glass tubes under argon. Solvents (Sigma-Aldrich) were distilled from P_4O_{10} before use. Infrared spectra were recorded at 298 K on a FT IR-Perkin Elmer Spectrometer, equipped with UATR sampling accessory. Magnetic susceptibilities (reported per W atom) were measured at 298 K on solid samples with a Magway MSB Mk1 magnetic susceptibility balance (Sherwood Scientific Ltd.). Diamagnetic corrections were introduced according to König.[1] NMR spectra were recorded on a Bruker Avance II DRX400 instrument equipped with BBFO broadband probe, at 298 K. The chemical shifts for ^{1}H and ^{13}C were referenced to the non-deuterated aliquot of the solvent. EPR spectra were recorded at 298 K on a Varian (Palo Alto, CA, USA) E112 spectrometer operating at X band, equipped with a Varian E257 temperature control unit and interfaced to IPC 610/P566C industrial grade Advantech computer, using acquisition board [2] and software package especially designed for EPR experiments.[3] Experimental EPR spectra were simulated by the WINSIM 32 program.[4] GC-MS analyses were performed on a HP6890 instrument, interfaced with MSD-HP5973 detector and equipped with a Phenonex Zebron column. Carbon, hydrogen and nitrogen analyses were performed on Carlo Erba mod. 1106 instrument. The chloride content was determined by the Mohr method [5] on solutions prepared by dissolution of the solid in aqueous KOH at boiling temperature, followed by cooling down to room temperature and addition of HNO_3 up to neutralization.

Reaction of WCl_6 with benzophenone imine, $Ph_2C=NH$: synthesis and characterization of $[Ph_2C=N=CPh_2][WCl_6]$, 1, and $[Ph_2C=NH_2][WCl_6]$, 2.

A suspension of WCl_6 (370 mg, 0.933 mmol) in 1,2-dichloroethane (ca. 15 mL) was heated to ca. 80 °C, and then benzophenone imine (0.31 mL, 1.9 mmol) was added. The mixture was left stirring for 12 h, then it was cooled to room temperature and the volatile materials were removed in vacuo. A dark residue was obtained which was washed with pentane (20 mL) and dried in vacuo. NMR

[1] E. König, *Magnetische Eigenschaften der Koordinations- und Metallorganischen Verbindungen der Übergangselemente in Landolt-Börnstein, Zahlenwerte und Funktionen aus Naturwissenschaften und Technik*, 6th Ed., Springer-Verlag, Berlin, Göttingen, Heidelberg, 1966, **2**, 16.
[2] R. Ambrosetti and D. Ricci, *Rev. Sci. Instrum.* 1991, **62**, 2281-2287.
[3] C. Pinzino and C. Forte, EPR-ENDOR, ICQEM-CNR Rome, Italy 1992.
[4] D. R. Duling, *J. Magn. Reson. B* 1994, **104**, 105-110.
[5] D. A. Skoog and D. M. West, *Fundamentals of Analytical Chemistry*, 2nd Edition, Holt, Rinehart and Winston, Chatham, UK, 1974, 233.

analysis of the residue (in CD_2Cl_2) evidenced the presence of **1** and **2**, with a slight prevalence of the latter. ^{1}H NMR (CD_2Cl_2): δ = 11.99 (s, NH_2, **2**); 7.98-7.94, 7.91-7.80, 7.65-7.37 ppm (m, Ph). ^{13}C NMR (CD_2Cl_2): δ = 182.6 (C=N, **2**);[6] 157.0 (C=N=C, **1**); 136.8, 135.3, 134.7, 133.2, 132.9, 132.4, 131.9, 131.8, 131.4, 130.6, 130.1, 129.8, 129.6, 129.5, 128.8, 128.4, 128.2, 127.3 ppm (Ph). Crystallization from CH_2Cl_2/hexane at −30 °C afforded a crop of crystals of both **1** (orange) and **2** (dark red-brown), which were mechanically separated.

1. Yield: 208 mg, 30%. Anal. Calcd. for $C_{26}H_{20}Cl_6NW$: C, 42.03; H, 2.71; N, 1.89; Cl, 28.63. Found: C, 41.81; H, 2.93; N, 1.76; Cl, 28.31. IR (solid state, cm^{-1}): ν = 1860m, 1846m-sh, 1826m-sh cm^{-1} (C=N=C).[7] Magnetic measurement: $\chi_M^{corr} = 3.54\times10^{-4}$ cgsu, $\mu_{eff} = 0.92$ BM.

2. Yield: 189 mg, 35%. Anal. Calcd. for $C_{13}H_{12}Cl_6NW$: C, 26.98; H, 2.09; N, 2.42; Cl, 36.75. Found: C, 27.16; H, 1.96; N, 2.57; Cl, 36.40. IR (solid state, cm^{-1}): ν = 3056w (N–H), 1645m-s (C=N). Magnetic measurement: $\chi_M^{corr} = 3.74\times10^{-4}$ cgsu, $\mu_{eff} = 0.95$ BM.

Reaction of $NOBF_4$ with benzophenone imine, Ph_2C=NH: identification of $[Ph_2C$=NH$][BF_4]$, 3, and $[Ph_2C$=$NH_2][BF_4]$.

A solution of benzophenone imine (0.10 mL, 0.60 mmol) in CH_2Cl_2 (10 mL) was treated with $NOBF_4$ (70 mg, 0.60 mmol). The resulting solution progressively turned violet; after 15 minutes reaction, an aliquot (0.05 mL) of the violet solution was withdrawn, conserved at 273 K and then analyzed by EPR at 293 K (see FIgure SI1). The remaining solution was stirred for additional 18 h, then hexane was added to the final colourless solution (30 mL). The resulting pale yellow solid, corresponding to $[Ph_2C$=$NH_2][BF_4]$, was dried in vacuo. Yield 113 mg, 70%. Anal. Calcd. for $C_{13}H_{12}BF_4N$: C, 58.03; H, 4.50; N, 5.21. Found: C, 58.20; H, 4.38; N, 5.10. IR (solid state, cm^{-1}): ν = 3322m, 3160m, 1651m-s (C=N), 1595s, 1499w, 1454m, 1376s, 1286w, 1164w, 1099s, 1038s, 996s, 942m, 863m, 793s, 766m, 725m, 688vs.

Reaction of WCl_6 with *N*-benzylidene-*tert*-butylamine, PhCH=N^{t}Bu.

A) Synthesis and characterization of $[PhCH$=$NH^tBu][WCl_6]$, 4.

To a suspension of WCl_6 (513 mg, 1.29 mmol) in hexane (ca. 10 mL), *N*-benzylidene-*tert*-butylamine (0.23 mL, 1.3 mmol) was added. The mixture was left stirring for 12 h at room temperature, then the resulting brown precipitate was isolated and dried in vacuo. Yield 348 mg, 48%. Anal. Calcd. for $C_{11}H_{16}Cl_6NW$: C, 23.64; H, 2.89; N, 2.51; Cl, 38.07. Found: C, 23.48; H, 3.01; N, 2.35; Cl, 37.90. IR (solid state, cm^{-1}): ν = 3252w (N–H), 2978w, 1650s (C=N), 1595m-s, 1455w-m, 1415w, 1382m, 1330w, 1311w, 1237m, 1187m-s, 1166w-m, 1024s, 999w, 824w-m,

[6] B. Samuel, R. Snaith, C. Summerford and K. Wade, *J. Chem. Soc. A* 1970, 2019-2022.
[7] M. Al-Talib and J. C. Jochims, *Chem. Ber.* 1984, **117**, 3222-3230.

745vs, 698w, 673s. Magnetic measurement: χ_M^{corr} = 2.90·10^{-4} cgsu, μ_{eff} = 0.84 BM. ^{1}H NMR (CD_3CN): δ = 10.85 (m, 1 H, $^3J_{HH}$ = 17.6 Hz, NH); 8.77 (d, 1 H, $^3J_{HH}$ = 17.6 Hz, CH); 8.10, 7.93, 7.75 (m, 5 H, Ph); 1.62 ppm (s, 9 H, CMe_3). ^{13}C NMR (CD_3CN): δ = 168.6 (C=N); 142.2 (ipso-Ph); 138.1, 132.6, 130.5 (Ph); 62.5 (*C*Me$_3$); 27.8 ppm (C*Me*$_3$).

B) Identification of PhC≡N and evidence for the formation of [PhC≡N^{t}Bu]$^+$. The reaction of WCl_6 (0.45 mmol) with *N*-benzylidene-*tert*-butylamine (0.45 mmol) was carried out in CD_2Cl_2 (2 mL), by following a procedure analogous to that described for the isolation of **4**. The resulting red solution was separated from an abundant green-brown precipitate and analyzed by NMR. ^{1}H NMR (CD_2Cl_2): δ = 10.50 (br, NH); 8.90, 8.37 (s-br, CH); 7.93-7.26 (m, Ph); 4.50 (s); 1.75, 1.60 (s, CMe_3) ppm. ^{13}C NMR (CD_2Cl_2): δ = 168.9 (C=N); 146.8, 140.7, 137.5, 135.0, 132.5, 131.5, 130.8-127.8 (Ph); 121.4, 112.4, 110.9; 69.6, 65.0 (*C*Me$_3$); 36.1, 31.3 ppm (C*Me*$_3$). Then, the solution was dried in vacuo and the red residue was analyzed by IR spectroscopy. IR (solid state, cm^{-1}): ν = 2267s, 2250w-sh, 2229w (C≡N), 1657s (C=N). NMR analysis of the precipitate revealed the presence of **4** as the prevalent species.

In a different experiment, WCl_6 (0.60 mmol) and *N*-benzylidene-*tert*-butylamine (0.60 mmol) were allowed to react in $CDCl_3$ (3 mL), for 18 h. The resulting mixture was treated with an aqueous solution of $NaHCO_3$ (6.3 mmol). After 48 h stirring, the orange organic phase was separated from a colourless solution and analyzed by ^{1}H and ^{13}C NMR spectroscopy, and GC-MS. PhCH=O, PhCH=N^{t}Bu and PhCN were detected in ca. 1:1:1 ratio.[8,9]

Gas-Chromatographic analyses. Samples for gas chromatographic analyses were prepared as follows: a mixture of WCl_6 (ca. 1 mmol) and the appropriate imine (ca. 2 mmol) in CH_2Cl_2 (10 mL) was stirred at room temperature for 48 h in a Schlenk tube tapped with a silicon stopper. Then an aliquot of the reaction atmosphere was withdrawn by a 1 mL syringe through the stopper, and injected into the GC instrument. The yields of N_2 formation were estimated based on analyses of gaseous standard mixtures containing known amounts of N_2. From WCl_6/benzophenone imine: 25%; from WCl_6/2,2,4,4-tetramethyl-3-pentanone imine: 7%; from WCl_6/*N*-benzylidene-*tert*-butylamine: not detected. A blank experiment carried out with benzophenone imine in the absence of WCl_6 led to the non detection of N_2.

[8] The treatment of the reaction mixture with a weakly basic water solution facilitates the release of the organic compounds from the highly oxophilic metal products, and allows the spectroscopic identification of the former. As blank experiments, we have made *N*-benzylidene-*tert*-butylamine (0.5 mmol) to interact with a mixture of WCl_6 (0.5 mmol), $CDCl_3$ (1.5 mL) and $KHCO_3$(aq) (ca. 10 mmol in 0.3 mL solution). The amines were generally identified by NMR as unique organic compounds in the resulting solutions.

[9] S. Dolci, F. Marchetti, G. Pampaloni and S. Zacchini, *Dalton Trans.* 2010, **39**, 5367-5376.

X-ray crystallography.

The diffraction experiment was carried out on a Bruker APEX II diffractometer equipped with a CCD detector and using Mo-Kα radiation (Table SI1). Data were corrected for Lorentz polarization and absorption effects (empirical absorption correction SADABS [10]). The structure was solved by direct methods and refined by full-matrix least-squares based on all data using F^2.[11] H-atoms were placed in calculated positions and treated isotropically using the 1.2 fold U_{iso} value of the parent atom. All non-hydrogen atoms were refined with anisotropic displacement parameters. The crystals of **1·CH$_2$Cl$_2$** are non-merohedrally twinned. The TwinRotMat routine of PLATON [12] was used to determine the twinning matrix and to write the reflection data file (.hkl) containing two twin components. Refinement was performed using the instruction HKLF 5 in SHELXL and one BASF parameter. Because of this twinning problem, the value of the weighted R factor is rather high as indicated by an ALERT A in the checkcif.

Table SI1. Crystal data and experimental details for **1·CH$_2$Cl$_2$**.

Formula	$C_{27}H_{22}Cl_8NW$
Fw	827.91
T, K	100(2)
λ, Å	0.71073
Crystal system	Triclinic
Space group	$P\bar{1}$
a, Å	10.179(13)
b, Å	13.62(2)
c, Å	14.88(3)
α, °	114.57(3)
β, °	100.377(16)
γ, °	101.214(15)
Cell Volume, Å^3	1759(5)
Z	2
D_c, g cm^{-3}	1.563
μ, mm^{-1}	3.908
F(000)	802
Crystal size, mm	0.16×0.13×0.10
θ limits, °	1.57–25.03
Reflections collected	14039
Independent reflections	6025 [R_{int}= 0.1563]
Data / restraints /parameters	6053 / 210 / 424
Goodness on fit on F^2	1.335
R_1 (I> 2σ(I))	0.1915
wR_2 (all data)	0.4749
Largest diff. peak and hole, e Å^{-3}	4.781 / –6.476

[10] G. M. Sheldrick, *SADABS*, *Program for empirical absorption correction*, University of Göttingen, Göttingen, Germany, 1997.

[11] G. M. Sheldrick, *SHELX97*, *Program for crystal structure determination*, University of Göttingen, Göttingen, Germany, 1997.

[12] A. L. Spek, PLATON, A Multipurpose Crystallographic Tool, Utrecht University, Utrecht, The Netherlands, 2005.

Figure SI1. EPR spectrum of $[Ph_2CNH][BF_4]$, **3**: A) experimental (CH_2Cl_2, 293 K), B) calculated.

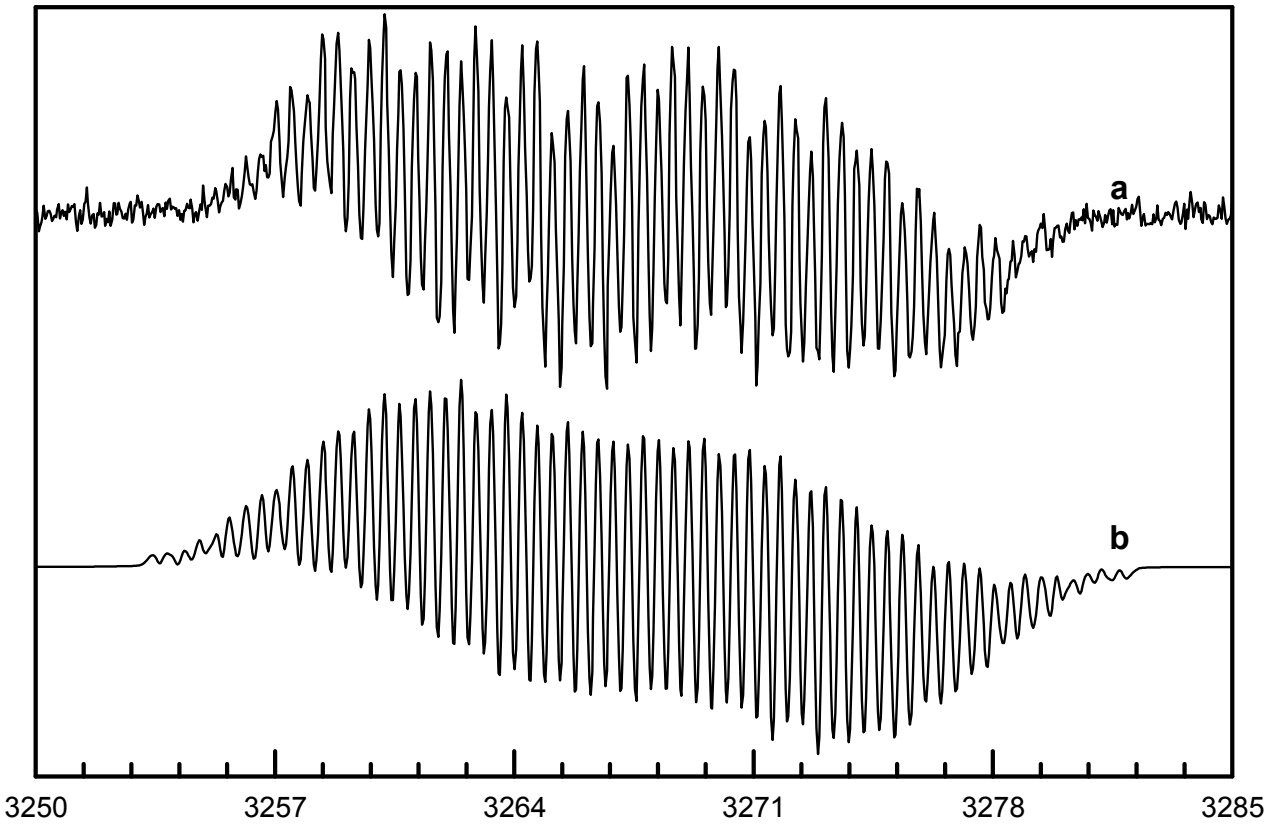

Line width = 0.17

Lorentzian = 45%

g_{iso} = 2.0035

Hyperfine coupling constant

Set	*Coupling*	*Spin*	*Number*
1	5.31	1	1
2	3.61	0.5	1
3	2.680	0.5	1
4	2.260	0.5	1
5	2.190	0.5	1
6	1.860	0.5	1
7	1.300	0.5	1
8	1.299	0.5	1
9	0.980	0.5	1
10	0.590	0.5	1
11	0.500	0.5	1
12	0.320	0.5	1

Electrochemical studies. Electrochemical measurements were recorded on a Princeton Applied Research (PAR) 273A Potentiostat/Galvanostat, interfaced to a computer employing PAR M270 electrochemical software, and performed in CH_2Cl_2 solutions containing $[N^nBu_4][PF_6]$ (0.2 mol dm^{-3}) as the supporting electrolyte at room temperature (20±5 °C). HPLC grade CH_2Cl_2 (Sigma-Aldrich) was stored under argon over 3-Å molecular sieves. Electrochemical grade $[N^nBu_4][PF_6]$ was purchased from Fluka and used without further purification. Ferrocene ($FeCp_2$) was prepared according to literature.[13] Cyclic voltammetry was performed in a three-electrode cell, having a platinum-disc working electrode, a platinum-spiral counter electrode and a quasi-reference electrode of platinum. After recording a sufficient number of voltammograms, a small amount of ferrocene was added to the solution and a further voltammogram was recorded. Under the present experimental conditions, the one-electron oxidation of ferrocene occurs at E° = +0.39 V *vs* SCE.

Infrared (IR) and ultraviolet (UV-vis) spectroelectrochemical measurements were carried out using an optically transparent thin-layer electrochemical (OTTLE) cell equipped with CaF_2 windows, platinum mini-grid working and auxiliary electrodes and silver wire pseudo-reference electrode.[14] During the microelectrolysis procedures, the electrode potential was controlled by a Princeton Applied Research (PAR) 273A Potentiostat/Galvanostat, interfaced to a computer employing PAR M270 electrochemical software. Argon-saturated CH_2Cl_2 solutions of the compound under study, containing $[N^nBu_4][PF_6]$ 0.2 M as the supporting electrolyte, were used.

The *in situ* spectroelectrochemical experiments were performed by collecting IR/UV-vis spectra at constant time intervals during the oxidation, obtained by continuously increasing the initial working potential by a 1.0 mV/sec scan rate. IR spectra were recorded on a Perkin-Elmer FT-IR 1725X spectrophotometer and UV-vis spectra on a Perkin-Elmer Lambda EZ201 spectrophotometer.

[13] G. Wilkinson, *Org. Synth.* 1956, **36**, 31-34.
[14] M. Krejčik, M. Daněk and F. Hartl, *J. Electroanal. Chem.* 1991, **317**, 179-187.

Figure SI2. UV-vis spectra of $Ph_2C{=}NH$ in CH_2Cl_2 solution, containing $[N^nBu_4][PF_6]$ (0.2 mol dm^{-3}) as the supporting electrolyte, recorded in an OTTLE cell as the potential is increased anodically from 0.0 to 2.0 V. The absorptions of the solvent and the supporting electrolyte have been subtracted.

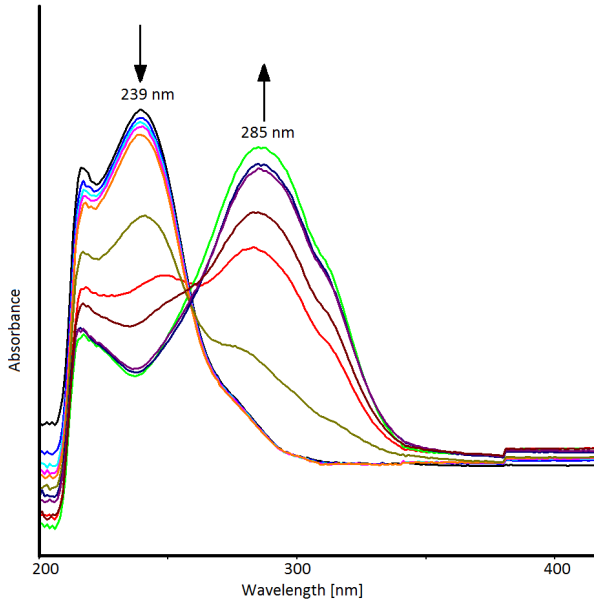

Figure SI3. (a) IR spectral changes recorded in an OTTLE cell as the potential of a CH_2Cl_2 solution of $Ph_2C{=}NH$ is anodically increased from 0.0 to 2.0 V. $[N^nBu_4][PF_6]$ (0.2 mol dm^{-3}) as the supporting electrolyte. The absorptions of the solvent and the supporting electrolyte have been subtracted. (b) IR spectrum of $[Ph_2C{=}NH_2][BF_4]$ in a $CH_2Cl_2/[N^nBu_4][PF_6]$ solution.

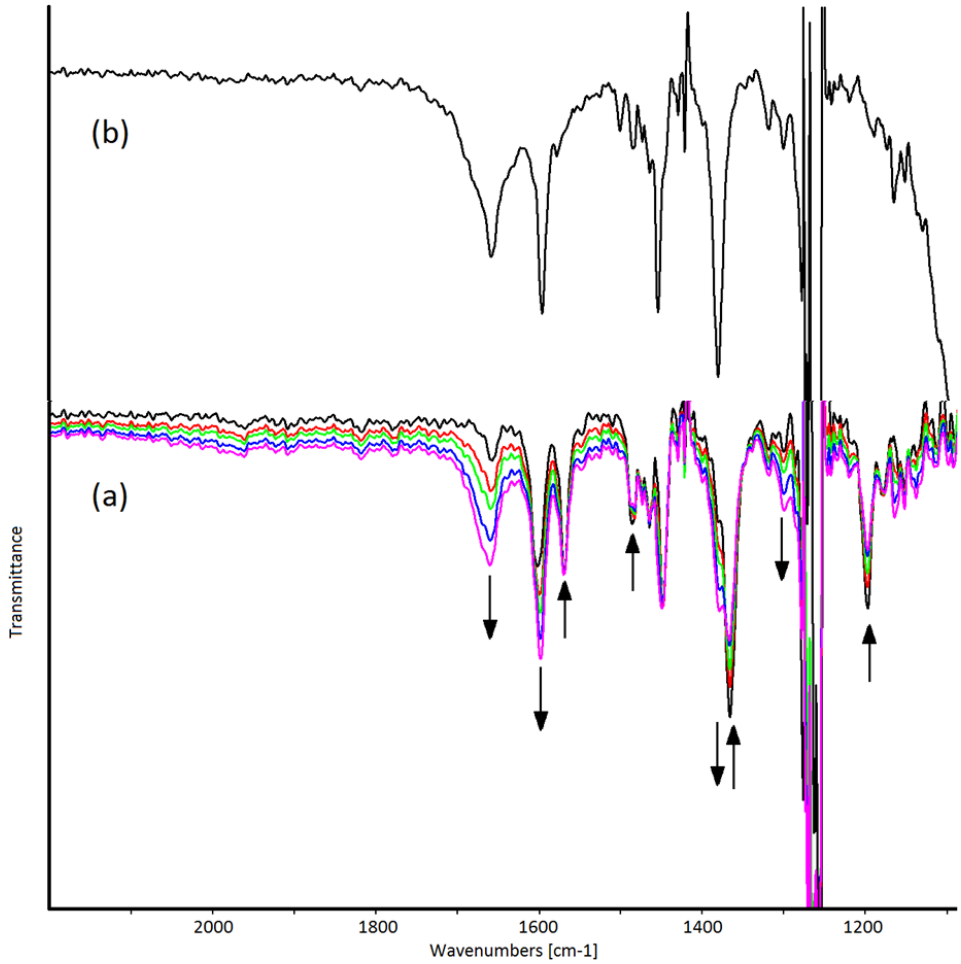

Figure SI4. UV-vis spectra of PhCH=N^{t}Bu in CH_2Cl_2 solution, containing [N^{n}Bu$_4$][PF_6] (0.2 mol dm^{-3}) as the supporting electrolyte, recorded in an OTTLE cell as the potential is anodically increased from 0.0 to 2.0 V. The absorptions of the solvent and the supporting electrolyte have been subtracted.

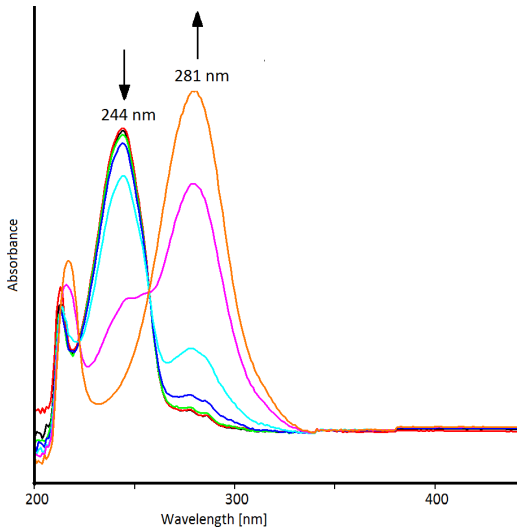

Figure SI5. (a) IR spectral changes recorded in an OTTLE cell as the potential of a CH_2Cl_2 solution of PhCH=N^{t}Bu is anodically increased from 0.0 to 2.0 V. [N^{n}Bu$_4$][PF_6] (0.2 mol dm^{-3}) as the supporting electrolyte. The absorptions of the solvent and the supporting electrolyte have been subtracted. (b) IR spectrum of [PhCH=NH^{t}Bu][BF_4] in a CH_2Cl_2/[N^{n}Bu$_4$][PF_6] solution.

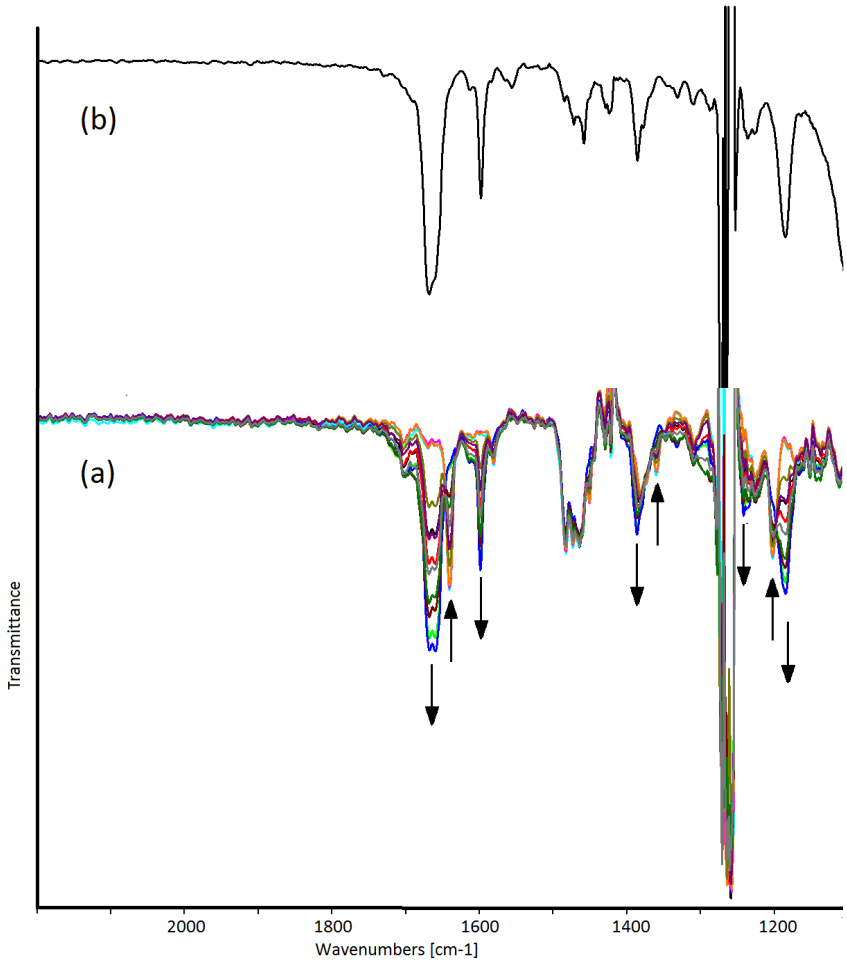

Computational studies.

The computational geometry optimizations were carried out without symmetry constrains, using the hybrid-GGA EDF2 functional [15] in combination with the 6-31G** basis set (ECP-based LANL2DZ basis set for elements beyond Kr).[16] The "unrestricted" formalism was applied for compounds with unpaired electrons, and the lack of spin contamination was verified by comparing the computed $<S^2>$ values with the theoretical ones. The stationary points were characterized by IR simulations (harmonic approximation), from which zero-point vibrational energies and thermal corrections (T = 298.15 K) were obtained.[17] Further optimization of selected geometries was carried out using the range-separated DFT functional ωB97X,[18] in combination with the split-valence polarized basis set of Ahlrichs and Weigend, with ECP on the metal centre.[19] The C-PCM implicit solvation model (ε = 9.08) was added to ωB97X calculations.[20] The software used for C-PCM/ωB97X calculations was Gaussian '09,[21] while EDF2 calculations were performed with Spartan '08.[22]

[15] C. Y. Lin, M. W. George and P. M. W. Gill, *Aust. J. Chem.* 2004 **57**, 365-370.

[16] (a) M. Dolg, *Modern Methods and Algorithms of Quantum Chemistry*, J. Grotendorst Ed., John Neumann Institute for Computing, NIC series, Jülich, 2000, **1**, 479. (b) P. J. Hay and W. R. Wadt, *J. Chem. Phys.* 1985, **82**, 270-283. (c) P. J. Hay and W. R. Wadt, *J. Chem. Phys.* 1985, **82**, 299-310. (d) W. J. Henre, R. Ditchfield and J. A. Pople, *J. Chem. Phys.* 1972, **56**, 2257-2261.

[17] C. J. Cramer, *Essentials of Computational Chemistry*, 2nd Edition, Wiley, Chichester, 2004.

[18] (a) Yu. Minenkov, Å Singstad, G. Occhipinti and V. R. Jensen, *Dalton Trans.* 2012, **41**, 5526-5541. (b) J.-D. Chai, M. Head-Gordon, *Phys. Chem. Chem. Phys.* 2008, **10**, 6615-6620. (c) I. C. Gerber and J. G. Ángyán, *Chem. Phys. Lett.* 2005, **415**, 100-105.

[19] (a) F. Weigend and R. Ahlrichs, *Phys. Chem. Chem. Phys.* 2005, **7**, 3297-3305. (b) D. Andrae, U. Haeussermann, M. Dolg, H. Stoll and H. Preuss, *Theor. Chim. Acta* 1990, **77**, 123-141.

[20] (a) M. Cossi, N. Rega, G.Scalmani and V. Barone, *J. Comput. Chem.* 2003, **24**, 669–681. (b) V. Barone and M. Cossi *J. Phys. Chem. A* 1998, **102**, 1995–2001.

[21] *Gaussian 09*, Revision C.01, M. J. Frisch et al., Gaussian, Inc., Wallingford CT, 2010.

[22] *Spartan '08*, version 1.1.1, Wavefunction, Inc., Irvine CA, 2009. Except for molecular mechanics and semi-empirical models, the calculation methods used in Spartan have been documented in: Y. Shao et al. *Phys. Chem. Chem. Phys.* 2006, **8**, 3172–3191.

Scheme SI6. Relative Gibbs energies of selected DFT-optimized intermediates (Figures SI13-SI16) along the proposed pathway for the decomposition of $[WCl_4N]^-$ into N_2 and $[WCl_6]^-$. C-PCM/ωB97X calculations.

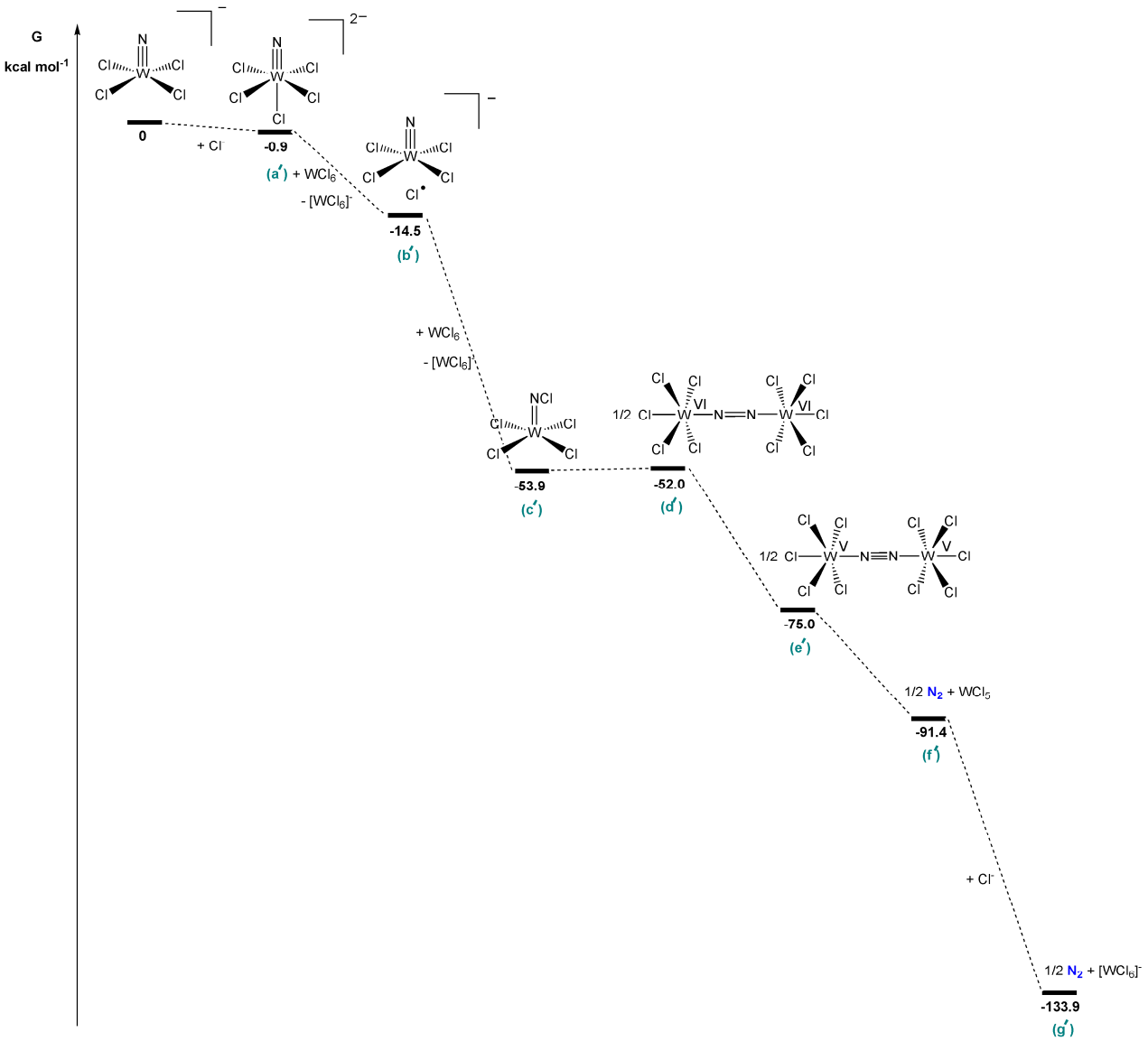

a´) ΔG = –0.9 kcal mol^{-1}

b´) ΔG, –13.6 kcal mol^{-1}. The geometry and spin density obtained for this step are in agreement with the oxidation of a chloride ligand to radical chlorine.

c´) Oxidation of $[WCl_4]^-$ by unreacted WCl_6 should afford the chloroimido complex $WCl_4(NCl)$, ΔG = –39.4 kcal mol^{-1}. The convergence to this stationary point can be ascribed to migration of Cl^+, formally generated in step b´, to the electron rich nitrogen atom.

d´) The interaction of two $WCl_4(NCl)$ molecules should result in a dinuclear species containing a bridging N_2 moiety, the N–N bond formation being accompanied by Cl migration to W (ΔG = +1.9 kcal mol^{-1}).

e´) The corresponding triplet state of the product, containing W(V) centres and N_2 as bridging ligand, is more stable by about 46 kcal mol^{-1}.

f´-g´) Decomposition of $W^VCl_5(\mu\text{-}N_2)W^VCl_5$ to WCl_5 and N_2 is thermodynamically favourable (ΔG = –32.8 kcal mol^{-1}), and further Gibbs free energy is liberated by the interaction of WCl_5 with chloride (ΔG = –42.5 kcal mol^{-1}).

Figure SI7. DFT-calculated structure of $Ph_2C(Cl)NH\text{-}WCl_5$ (C-PCM/wB97X calculations, dichloromethane as continuous medium). Selected computed bond lengths (Å) and angles (°): W–N 1.930; W–Cl (*trans* N) 2.352; W–Cl (*cis* N) 2.261, 2.322, 2.337, 2.343; N–H 1.026; C–N 1.472; C–Cl 1.829; N–W–Cl 83.9, 92.3, 93.4, 94.7, 172.1; N–C–Cl 102.8.

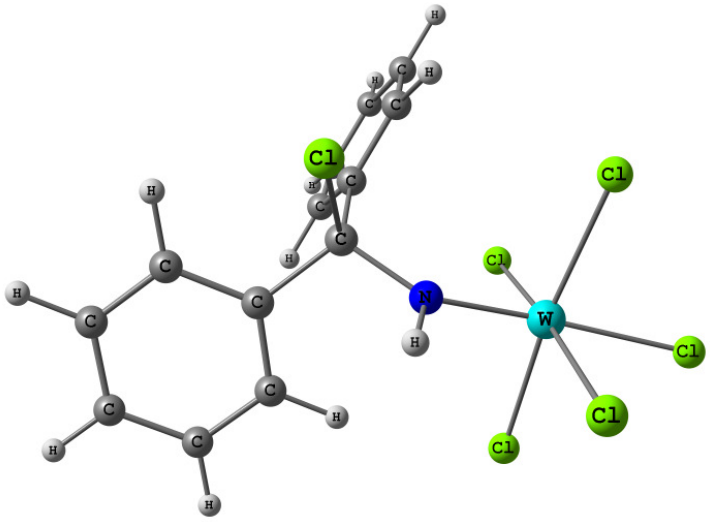

Figure SI8. DFT-calculated structure of $[WCl_5(NHCPh_2NHCPh_2)]Cl$ (EDF2 calulations). Hydrogen atoms on the phenyl rings have been omitted for clarity. Selected computed bond lengths (Å) and angles (°): W–N1 1.922; W–Cl (*trans* N1) 2.374; W–Cl (*cis* N) 2.284, 2.338, 2.346, 2.375; N1–H 1.074; N1–C 1.488; N2–C 1.503; N2–H 1.068; H---Cl 1.894, 2.003; N–W–Cl 88.6, 90.2, 93.7, 93.8, 176.5; N1–C–N2 103.1.

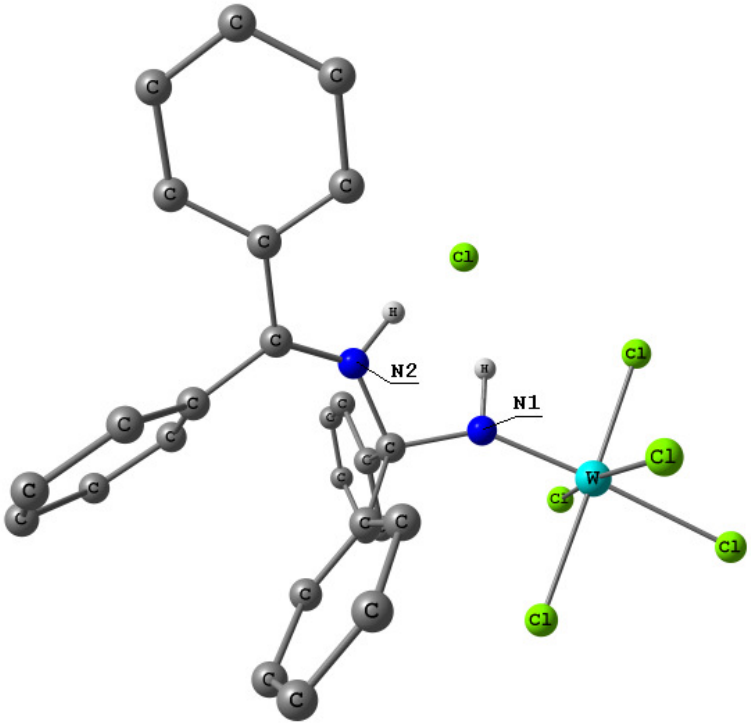

Figure SI9. DFT-calculated structure of $WCl_5(NCPh_2NHCPh_2)$ (C-PCM/wB97X calculations, dichloromethane as continuous medium). Hydrogen atoms on the phenyl rings have been omitted for clarity. Selected computed bond lengths (Å) and angles (°):W–N1 1.726; W–Cl (*trans* N1) 2.491; W–Cl (*cis* N) 2.347, 2.360, 2.364, 2.394; N1–C 1.432; N2–C 1.499; N2–H 1.020; N–W–Cl 89.8, 93.9, 96.8, 96.9; N1–C–N2 108.4.

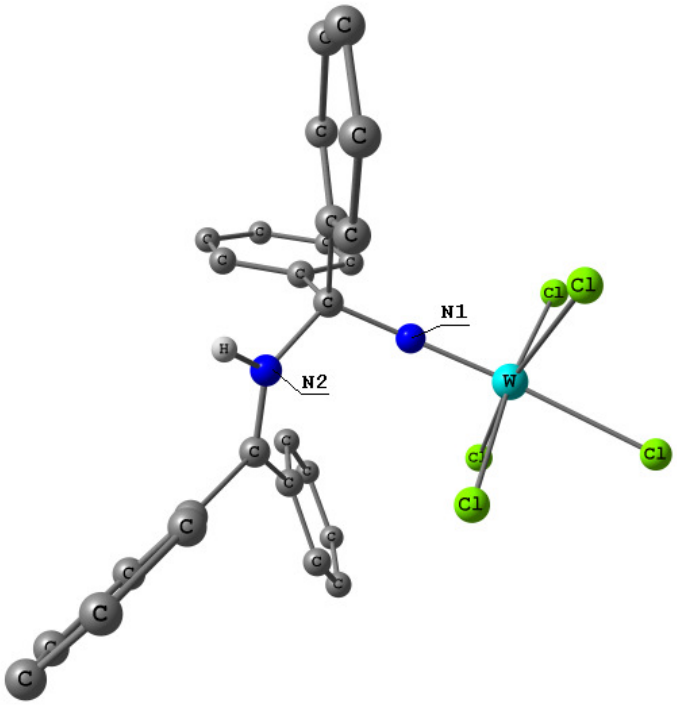

Figure SI10. DFT-calculated structure of $WCl_5(NHCPh_2NCPh_2)$ (C-PCM/wB97X calculations, dichloromethane as continuous medium). Hydrogen atoms on the phenyl rings have been omitted for clarity. Selected computed bond lengths (Å) and angles (°):W–N1 1.916; W–Cl (*trans* N1) 2.362; W–Cl (*cis* N) 2.259, 2.336, 2.339, 2.353; N1–H 1.025; N1–C 1.498; N2–C 1.450; N–W–Cl 81.7, 94.3, 94.9, 95.0, 167.0; N1–C–N2 108.7.

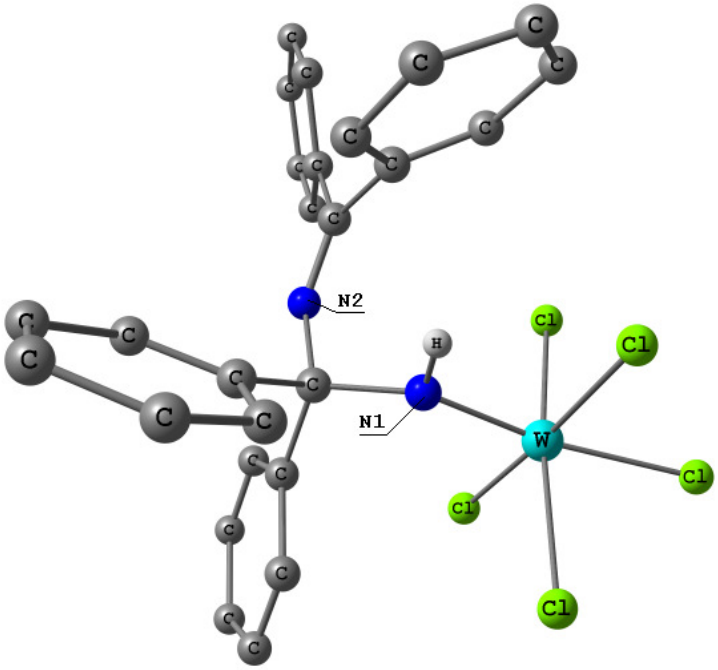

Figure SI11. DFT-calculated structure of $[Ph_2C{=}N{=}CPh_2][WCl_5NH]$ (C-PCM/wB97X calculations, dichloromethane as continuous medium). Hydrogen atoms on the phenyl rings have been omitted for clarity. Selected computed bond lengths (Å) and angles (°):W–N 1.704; W–Cl (*trans* N) 2.539; W–Cl (*cis* N) 2.357, 2.361, 2.372, 2.389; N–H 1.020; N–C 1.268, 1.269; N–W–Cl 94.2, 94.2, 95.5, 95.8, 178.1; C–N–C 173.9.

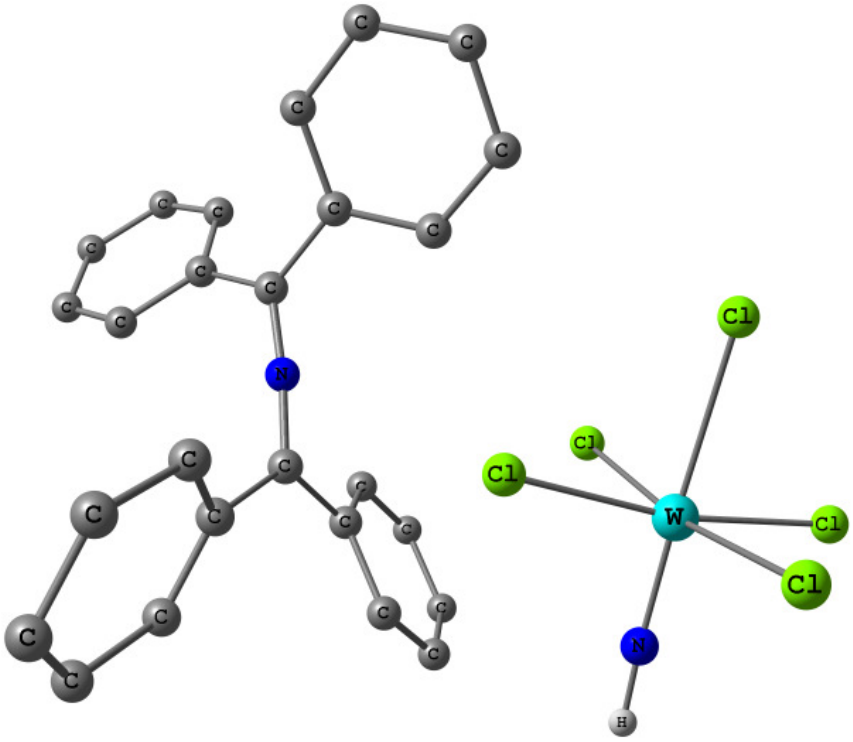

Figure SI12. DFT-calculated structure of $[WCl_4N]^-$ (C-PCM/wB97X calculations, dichloromethane as continuous medium). Selected computed bond lengths (Å) and angles (°): W–N 1.643; W–Cl 2.381, 2.386, 2.386, 2.390; N–W–Cl 99.8, 99.8, 100.3, 100.4.

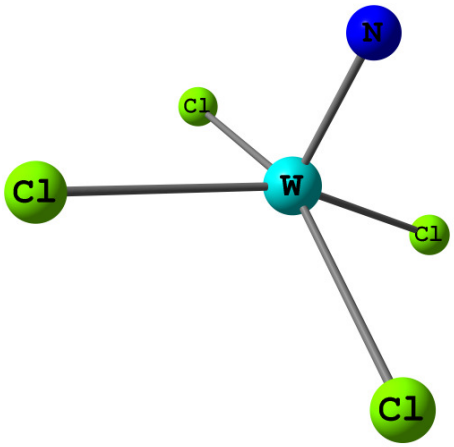

Figure SI13. DFT-calculated structure of $[WCl_5N]^{2-}$ (C-PCM/wB97X calculations, dichloromethane as continuous medium). Selected computed bond lengths (Å) and angles (°): W–N 1.658; W–Cl (*cis* N) 2.409, 2.409, 2.409, 2.409; W–Cl (*trans* N) 2.765; N–W–Cl 95.7, 95.7, 95.7, 95.7, 180.0.

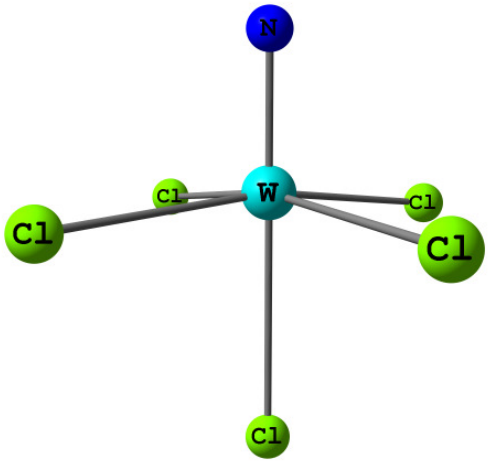

Figure SI14. DFT-calculated structure of $WCl_4(NCl)$ (C-PCM/wB97X calculations, dichloromethane as continuous medium). Selected computed bond lengths (Å) and angles (°): W–N 1.693; W–Cl 2.325, 2.328, 2.330, 2.331; N–Cl 1.618; W–N–Cl 179.8; N–W–Cl 100.4, 100.4, 101.0, 101.1.

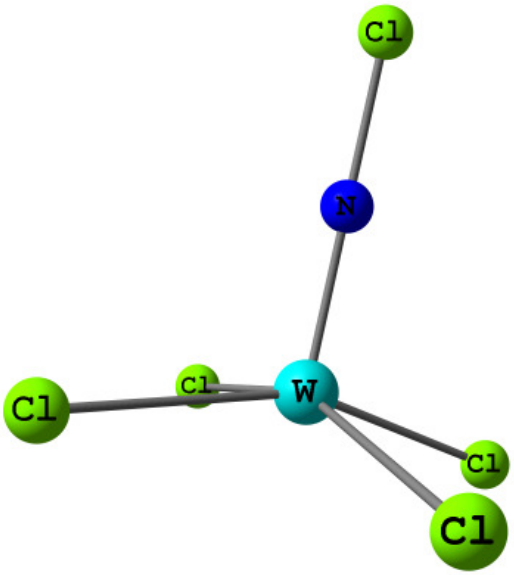

Figure SI15. DFT-calculated structure of $W^{VI}Cl_5(\mu\text{-}N_2)W^{VI}Cl_5$ (C-PCM/wB97X calculations, dichloromethane as continuous medium). Selected computed bond lengths (Å) and angles (°): W–N 2.026, 2.026; W–Cl 2.282, 2.282, 2.283, 2.283, 2.286, 2.286, 2.325, 2.325, 2.325, 2.325; N–N 1.136; W–N–N 178.3, 178.3; N–W–Cl 78.3, 78.3, 78.9, 78.9, 93.6, 93.6, 93.6, 93.6, 179.6, 179.6.

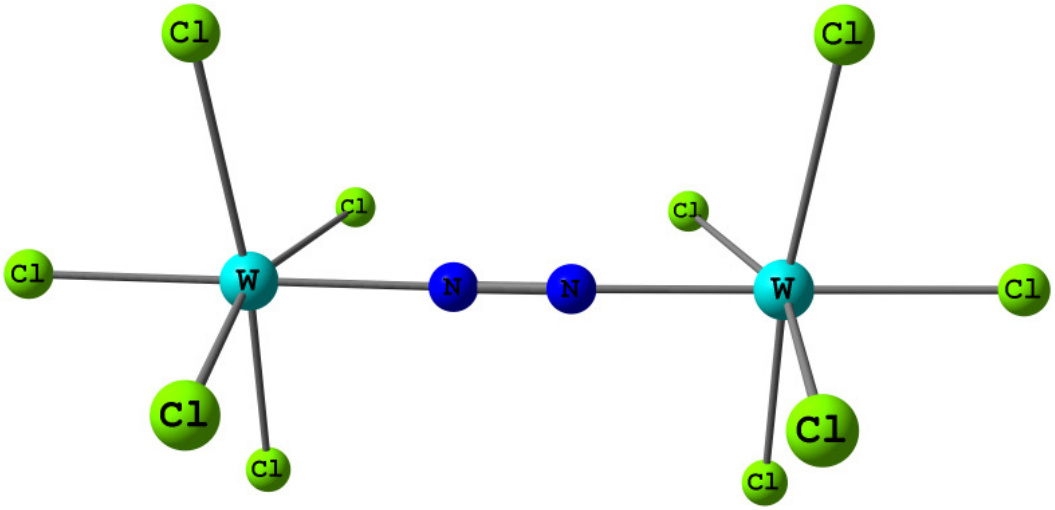

Figure SI16. DFT-calculated structure of $W^{V}Cl_5(\mu\text{-}N_2)W^{V}Cl_5$ (C-PCM/wB97X calculations, dichloromethane as continuous medium). Selected computed bond lengths (Å) and angles (°): W–N 2.813, 2.919; W–Cl 2.235, 2.236, 2.263, 2.265, 2.266, 2.269, 2.327, 2.332, 2.332, 2.332; N–N 1.094; W–N–N 180.0, 180.0; N–W–Cl 71.2, 71.2, 71.5, 71.8, 88.2, 88.5, 89.4, 90.1, 179.6, 179.9.

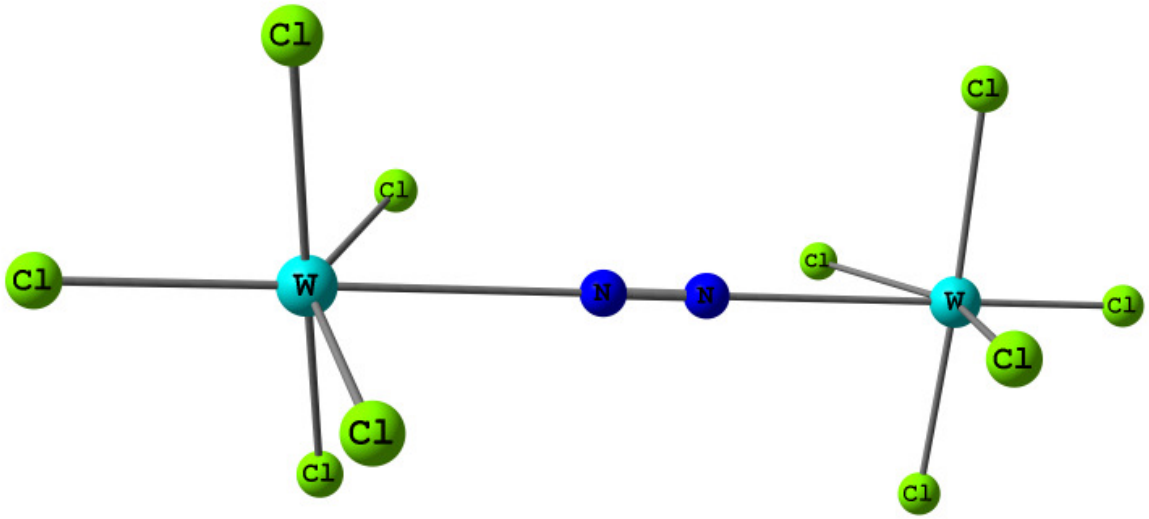

Figure SI17. DFT-calculated structure of $WCl_5(\kappa^2\text{-}C,N\text{-}PhC{=}N^tBu)$ (C-PCM/wB97X calculations, dichloromethane as continuous medium). Selected computed bond lengths (Å) and angles (°):W–N 2.103; W–C 2.103; W–Cl 2.309, 2.325, 2.356, 2.378, 2.398; N=C 1.241; C–W–N 34.3; C–N–C(^{t}Bu) 138.2; N–C–C(Ph) 141.5.

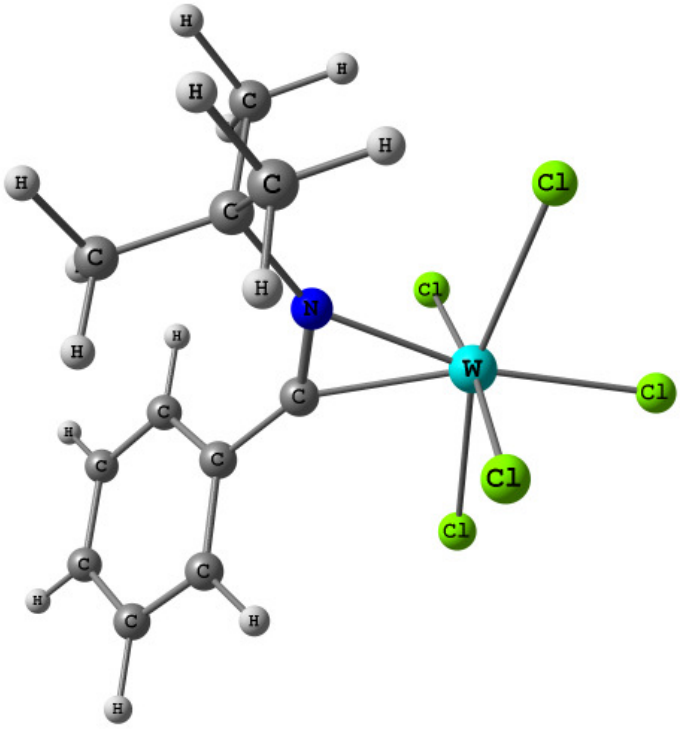

Figure SI18. DFT-calculated structure of $[PhC{\equiv}N^tBu][WCl_5]$ (C-PCM/wB97X calculations, dichloromethane as continuous medium). Selected computed bond lengths (Å) and angles (°):W–Cl 2.322, 2.332, 2.325, 2.419, 2.428; C≡N 1.148; N-C(tBu) 1.463; C–C(Ph) 1.426.